Hydrogen Evolution Reaction at Pd-Modified Nickel-Coated Carbon Fibre in 0.1 M NaOH Solution

Boguslaw Pierozynski[1,] and Ireneusz M. Kowalski[2]*

[1]Department of Chemistry, Faculty of Environmental Management and Agriculture, University of Warmia and Mazury in Olsztyn, Plac Lodzki 4, 10-957 Olsztyn, Poland
[2] Department of Rehabilitation, Faculty of Medical Sciences, University of Warmia and Mazury in Olsztyn, Zolnierska 14C Street, 10-561 Olsztyn, Poland
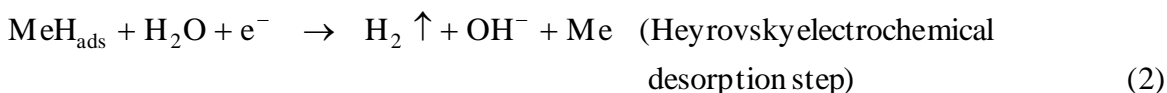[*]E-mail: bogpierozynski@yahoo.ca; boguslaw.pierozynski@uwm.edu.pl

The present paper reports on an electrochemical impedance study of hydrogen evolution reaction (HER), carried-out on "as received" and Pd-modified nickel-coated carbon fibre (NiCCF) materials. The HER was examined in 0.1 M NaOH solution for unmodified and electrochemically, Pd-deposited Toho-Tenax 12K50 NiCCF tow samples. Kinetics of the hydrogen evolution reaction were studied at room temperature (23 $^{\circ}$C) for the cathodic overpotential range: -50 to -400 mV vs. RHE. Corresponding values of charge-transfer resistance, exchange current-density and other electrochemical parameters for the examined catalyst materials were derived. Thus, Pd-modification of the NiCCF material (at near trace amount of palladium) led to a significant enhancement of its catalytic properties towards the HER.

Keywords: nickel-coated carbon fibre; NiCCF; HER; Pd-modification; impedance spectroscopy.

1. INTRODUCTION

Hydrogen evolution reaction (HER) at metal electrodes makes one of the most significant electrochemical processes, being especially important with respect to the development of PEM (Proton Exchange Membrane) fuel-cell and battery technologies [1]. So far, HER has extensively been studied on noble metal catalysts, especially such as polycrystalline and single-crystal surfaces of Pt [2-6], as well as on numerous other metals and their alloys, for example on Ni [7-10], Co [11], Pb [12], Zn-Ni [13], Ni-P [14, 15] and Ni-Mo [16]. Some recently published papers on the HER also covered examinations of nanostructural-type, carbon felt and glassy carbon-supported electrocatalysts [17-20].

Cathodic evolution of hydrogen leads to the formation of bulk H_2 species and proceeds at potentials negative to the H_2 reversible potential. The HER mechanism at metal (Me) electrode is based on a 2-step reaction, which involves an adsorbed H intermediate, as shown for an alkaline medium below [1, 2]:

$$H_2O + e^- + Me \quad \rightarrow \quad MeH_{ads} + OH^- \quad \text{(Volmer electrochemical disch arg e step)} \quad (1)$$

$$MeH_{ads} + H_2O + e^- \quad \rightarrow \quad H_2 \uparrow + OH^- + Me \quad \text{(Heyrovsky electrochemical}$$
$$\text{desorption step)} \quad (2)$$

$$2MeH_{ads} \quad \rightarrow \quad H_2 \uparrow + 2Me \quad \text{(Tafel catalytic recombination step)} \quad (3)$$

Current work makes a continuation of a series of earlier papers [21-24] on the kinetic aspects of the hydrogen evolution reaction at carbon fibre and nickel-coated carbon fibre materials that has recently been published from this laboratory. It primarily constitutes an a.c. impedance study of the HER, which is performed on unmodified, commercially available 12K50 NiCCF product and the Pd-modified 12K50 tow material in 0.1 M NaOH supporting electrolyte (compare with an analogous HER study, recently carried-out in 0.5 M H_2SO_4 and reported in Ref. 24). It should be stressed that nickel-coated carbon fibre could potentially serve as a source of large surface-area catalyst material, suitable for the commercial process of cathodic evolution of hydrogen. Of special importance are electrochemical (and chemical) modifications, which aim at enhancing the HER kinetics at trace amount of catalytic additives. Such-produced composite materials could potentially be employed to make large area (e.g. *woven* cathodes) for the generation of H_2 in commercial alkaline water electrolysers.

2. EXPERIMENTAL

2.1. Solutions and chemical reagents

All supporting electrolytes were prepared by means of a Direct-Q3 UV ultra-pure water purification system from Millipore. This system gives a final H_2O product of 18.2 MΩ cm resistivity. 0.1 M NaOH supporting solution was prepared from AESAR, 99.996 % (semiconductor grade) NaOH pellets. Atmospheric oxygen was removed from solution before each electrochemical experiment by bubbling with high-purity argon (Ar 6.0 grade, Linde). Also, during the experiments, the argon gas flow was kept above the solution.

2.2. Electrochemical cell, electrodes and experimental methodology

An electrochemical cell, made all of Pyrex glass, was used during the course of this work. The cell comprised three electrodes: a NiCCF (Toho-Tenax 12K50: 12,000 single filaments of about 7.5 μm diameter each and *ca*. 45 wt.% Ni) or Pd-modified NiCCF working electrode (WE) in a central part, a reversible Pd hydrogen electrode (RHE) as reference and a Pt counter electrode (CE), both placed in separate compartments. Before carrying-out the HER experiments (or prior to Pd

electrodeposition), all NiCCF tow electrodes were activated in 0.5 M H_2SO_4 by cathodic polarization at a current-density of 1 mA cm^{-2} for 600 s in order to remove any spontaneously formed oxide layer. Electrodeposition of Pd on NiCCF tow electrodes was carried-out from $PdCl_2$ (2 g dm^{-3}) solution of pH 1.5, at a cathodic current-density of 0.2 mA cm^{-2} for Pd loadings of *ca.* 1-2 wt.%. The palladium RHE was made of a coiled Pd wire (0.5 mm diameter, 99.9 % purity, Aldrich) and sealed in soft glass. Before its use, this electrode was cleaned in hot sulphuric acid, followed by cathodic charging with hydrogen in 0.5 M H_2SO_4, until H_2 bubbles in the electrolyte were clearly observed. The stability of the Pd reference electrode was occasionally checked by recording its potential shift in time. No significant potential shift was observed for such-prepared Pd reversible hydrogen electrode, up to three days from its initial charging with hydrogen. Thus, all the potentials throughout this work are given on the RHE scale. The counter electrode was made of a coiled Pt wire (1.0 mm diameter, 99.9998 % purity, Johnson Matthey, Inc.). Prior to its use, the counter electrode was cleaned in hot sulphuric acid. In the same way, before each series of experiments, the electrochemical cell was taken apart and soaked in hot sulphuric acid for at least 3 hours. After having been cooled to about 30 ^{o}C, the cell was thoroughly rinsed with Millipore ultra-pure water.

A.c. impedance spectroscopy and cyclic voltammetry electrochemical techniques were employed during the course of this work. All measurements were conducted at room temperature (23 ^{o}C) by means of the *Solartron* 12.608 W Full Electrochemical System, consisting of 1260 frequency response analyzer (FRA) and 1287 electrochemical interface (EI). For the impedance measurements, the generator provided an output signal of known amplitude: 5 mV and the frequency range was usually swept between 1.0×10^5 and 0.5×10^{-1} Hz. The instruments were controlled by *ZPlot 2.9* or *Corrware 2.9* software for Windows (Scribner Associates, Inc.). Presented impedance results were obtained through selection and analysis of representative series of experimental data. Typically, three impedance measurements were carried-out at each potential value, independently at several catalyst electrodes. Reproducibility of such-obtained results was usually below 10 % from tow-to-tow. Data analysis was performed with *ZView 2.9* (*Corrview 2.9*) software package, where the impedance spectra were fitted by means of a complex, non-linear, least-squares immitance fitting program, *LEVM 6*, written by J.R. Macdonald [25]. In addition, spectroscopic characterization of the Pd-modified NiCCF composite electrodes was performed by means of Quanta FEG 250 scanning electron microscope (SEM).

3. RESULTS AND DISCUSSION

3.1. Scanning electron microscopy characterization of Pd-modified NiCCF electrodes

For a Pd-modified nickel-coated carbon fibre electrode (at *ca.* 1.5 wt.% of palladium), an inhomogeneous catalyst deposit could scarcely be observed on individual NiCCF filaments, see Figs. 1a and 1b. In addition, the obtained Pd deposit was very coarse, as compared to that of Ni for the Toho-Tenax fibre. The above can clearly be seen in a highly-magnified SEM micrograph of Fig. 1c. The latter most likely results from the fact that a commercial, continuous process for the production of

Toho-Tenax 12K50 NiCCF composite is performed at significantly higher current-densities (and voltages) than the batch-type, laboratory Pd electrodeposition process employed in this work (see Experimental section 2.2 for details).
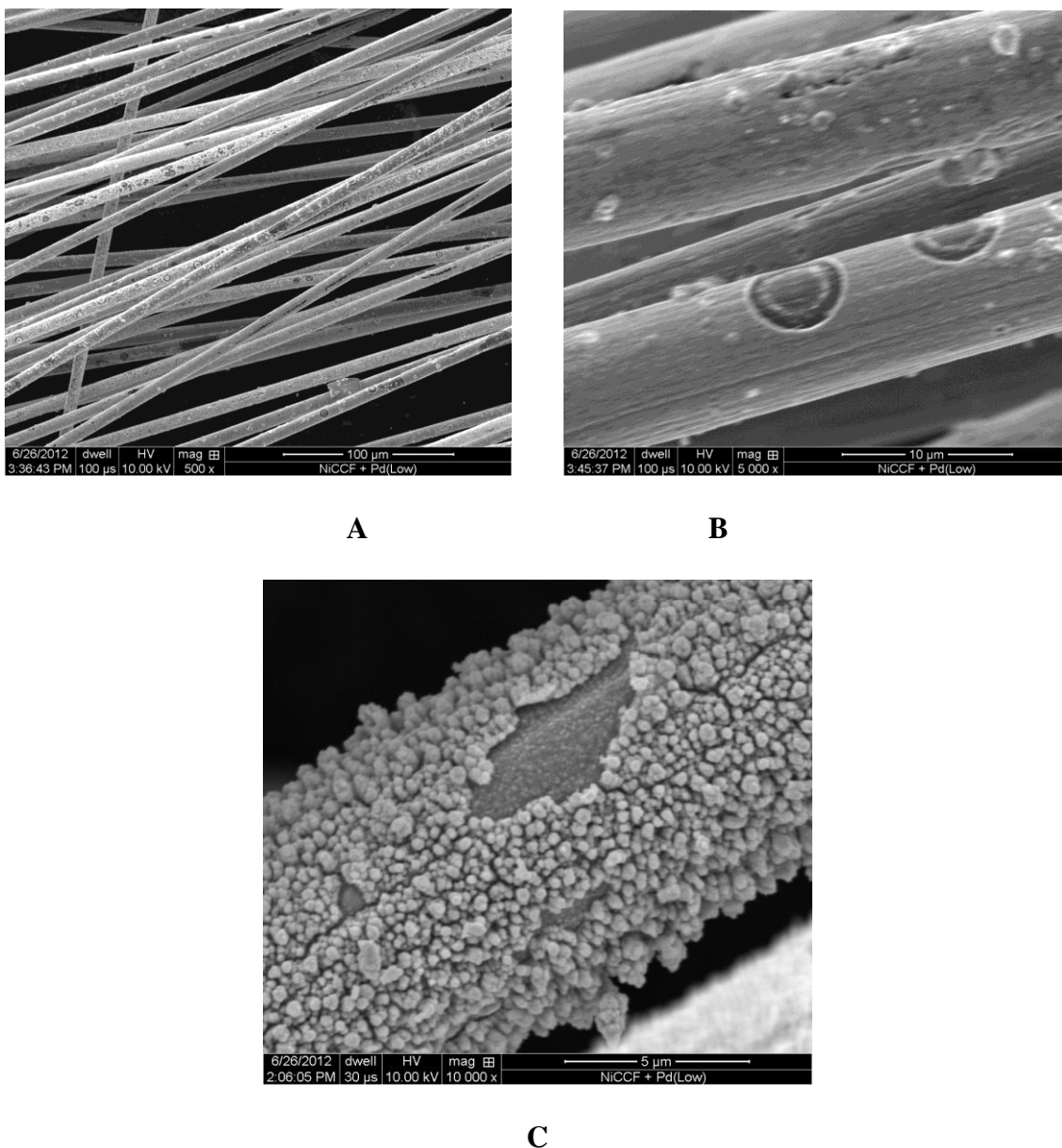

A   **B**

C

Figure 1. a) SEM micrograph picture of Pd-modified (*ca*. 1.5 wt.% Pd) Toho-Tenax 12K50 NiCCF tow sample, taken at 500 magnification. b) As in (a), but taken at 5,000 magnification. c) As in (a), but taken at 10,000 magnification.

3.2. Hydrogen evolution reaction on NiCCF and Pd-modified NiCCF tow electrodes in 0.1 M NaOH

The impedance behaviour of the HER at Toho-Tenax 12K50 NiCCF and Pd-modified NiCCF tow electrodes in 0.1 M NaOH is presented in Figs. 2a and 2b, correspondingly and in Table 1.

Table 1. Electrochemical parameters for the HER, obtained at Toho-Tenax and Pd-modified Toho-Tenax 12K50 NiCCF tow electrodes, in contact with 0.1 M NaOH. The results were obtained by fitting the two CPE-*R* element (Fig. 3) equivalent circuit to the experimentally obtained impedance data (reproducibility usually below 10 %, $\chi^2 = 6.7 \times 10^{-5}$ to 1.8×10^{-3}).

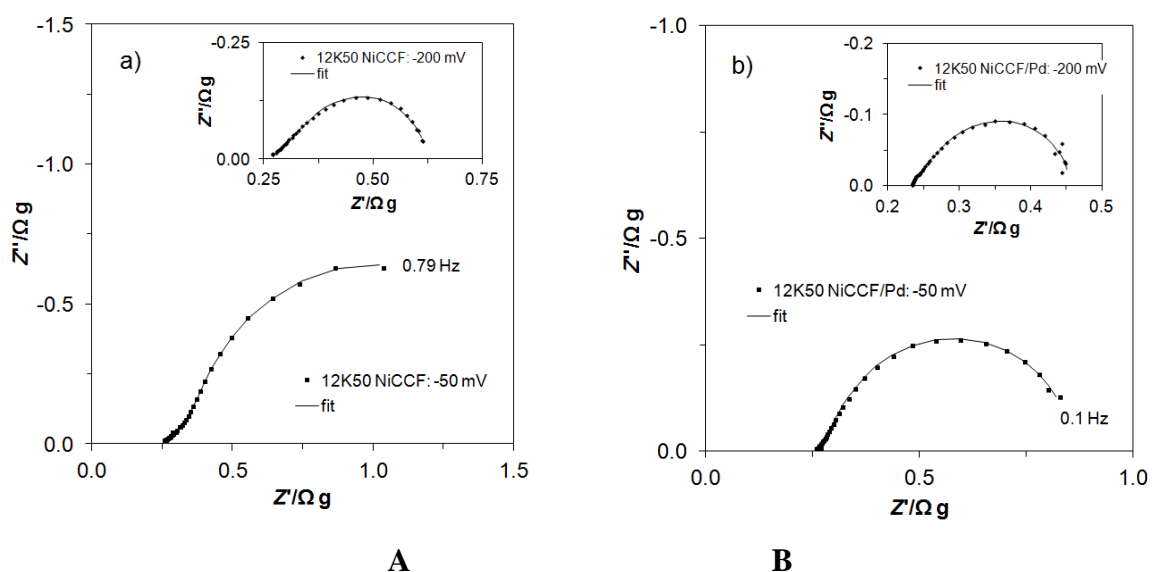| E/mV	R_{ct}/Ω g	$C_{dl}/\mu F\ g^{-1}s^{\varphi1-1}$	R_p/Ω g	$C_p/\mu F\ g^{-1}s^{\varphi2-1}$
	Toho-Tenax 12K50 NiCCF			
-50	1.230 ± 0.043	172,055 ± 3,544	0.258 ± 0.028	798,545 ± 72,677
-100	0.794 ± 0.042	155,198 ± 3,414	0.242 ± 0.019	613,968 ± 72,141
-200	0.230 ± 0.017	120,854 ± 4,194	0.138 ± 0.014	378,307 ± 33,795
-300	0.109 ± 0.009	126,116 ± 4,075	0.054 ± 0.006	232,902 ± 19,098
-400	0.072 ± 0.007	80,820 ± 9,779	0.022 ± 0.004	48,330 ± 7,733
	Pd-modified Toho-Tenax 12K50 NiCCF			
-50	0.517 ± 0.028	755,873 ± 33,258	0.094 ± 0.011	2,160,529 ± 272,226
-100	0.380 ± 0.033	744,365 ± 46,820	0.089 ± 0.011	2,259,338 ± 318,566
-200	0.145 ± 0.022	789,179 ± 75,761	0.081 ± 0.013	1,370,291 ± 230,209
-300	0.040 ± 0.006	740,926 ± 108,916	0.085 ± 0.015	669,286 ± 144,565
-400	0.020 ± 0.003	509,206 ± 74,853	0.057 ± 0.011	704,100 ± 121,105

Figure 2. a) Complex-plane impedance plots for "as received" Toho-Tenax 12K50 NiCCF tow electrode in contact with 0.1 M NaOH, recorded at room temperature for the stated potential values (vs. RHE). The solid lines correspond to representation of the data according to the equivalent circuit shown in Fig. 3. b) As in (a), but for Pd-modified NiCCF tow electrode.

Thus, both unmodified and the Pd-modified NiCCF catalyst materials exhibited two "depressed" partial semicircles at all examined potentials, in the explored frequency range (see examples of the recorded Nyquist impedance plots in Figs. 2a and 2b). Here, a circuit model containing two CPE-R elements was employed to characterize the obtained impedance behaviour (see Fig. 3). In this model, the high-frequency semicircle (CPE$_p$-R_p) corresponds to the porosity of the electrode, whereas the low-frequency semicircle (CPE$_{dl}$-R_{ct}) is related to the HER kinetics [10, 18-20].
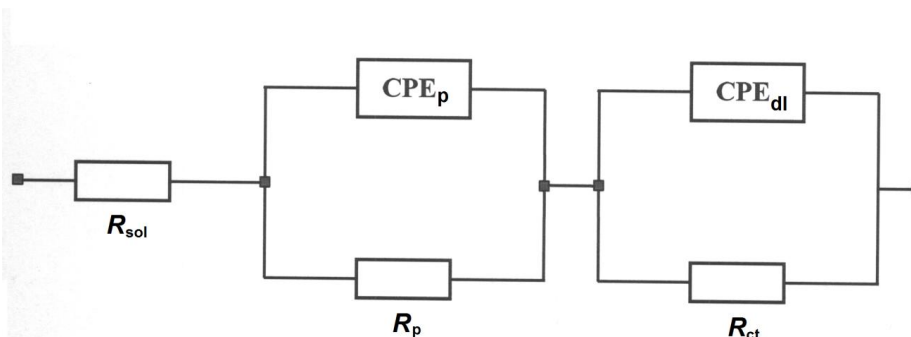

Figure 3. Two CPE-R element equivalent circuit model used for fitting the impedance data for "as received" and Pd-modified Toho-Tenax 12K50 NiCCF tow electrodes, obtained in 0.1 M NaOH solution. The circuit includes two constant phase elements (CPEs) to account for distributed capacitance; R_{ct} and C_{dl} (CPE$_{dl}$) elements correspond to the HER charge-transfer resistance and double-layer capacitance components; R_p and C_p (CPE$_p$) elements refer to the resistance and capacitance components of an electrode porosity response; R_{sol} is solution resistance.

The recorded charge transfer resistance parameter (R_{ct}) for the Toho-Tenax NiCCF electrode ranged from 1.230 Ω g at -50 mV to 0.072 Ω g at -400 mV vs. RHE. These results are in a good agreement with those previously published on this catalyst material in Ref. 21. On the other hand, a radius of the high-frequency semicircle (surface porosity impedance response) is considerably less overpotential-dependent, especially at initial potential values. Hence, the recorded R_p parameter in Table 1 diminished from 0.258 to 0.138 Ω g over the cathodic potential range: 50-200 mV (also refer to the respective values of pseudocapacitance parameter, C_p in Table 1).

On the other hand, Pd modification of the NiCCF material led to a significant reduction of the charge-transfer resistance parameter by nearly 2.4 and 3.6 times at the overpotential values of -50, and -400 mV, respectively (see Table 1 for details). The above behaviour is reflected in considerably different values of the exchange current-density parameter (calculated based on the Butler-Volmer equation, see e.g. Ref. 21) recorded for "as received" NiCCF and the Pd-modified NiCCF tow electrodes, which came to 7.9×10^{-6} and 1.4×10^{-5} A cm^{-2}, respectively (see Fig. 4). In contrast to the behaviour recorded at pure NiCCF composite, for the palladium-modified NiCCF electrode the porosity-related resistance parameter (R_p) exhibited relatively constant value of *ca.* 0.080-0.090 Ω g over the potential range: -50 to -300 mV vs. RHE (also refer to the corresponding values of the C_p parameter in Table 1). In other words, the Pd-modified fibre samples maintained higher tow's integrity

under the HER conditions than that exhibited by the Toho-Tenax fibre electrodes. Hence, the HER preferentially proceeds on the highly-active palladium sites.
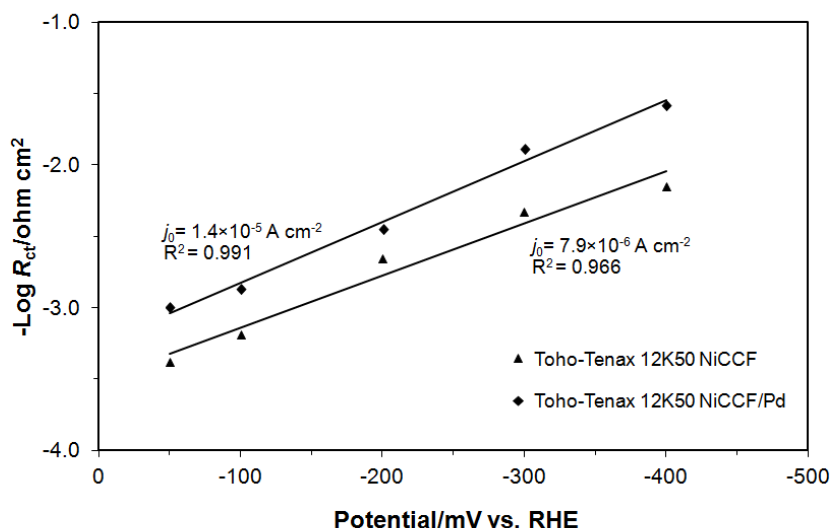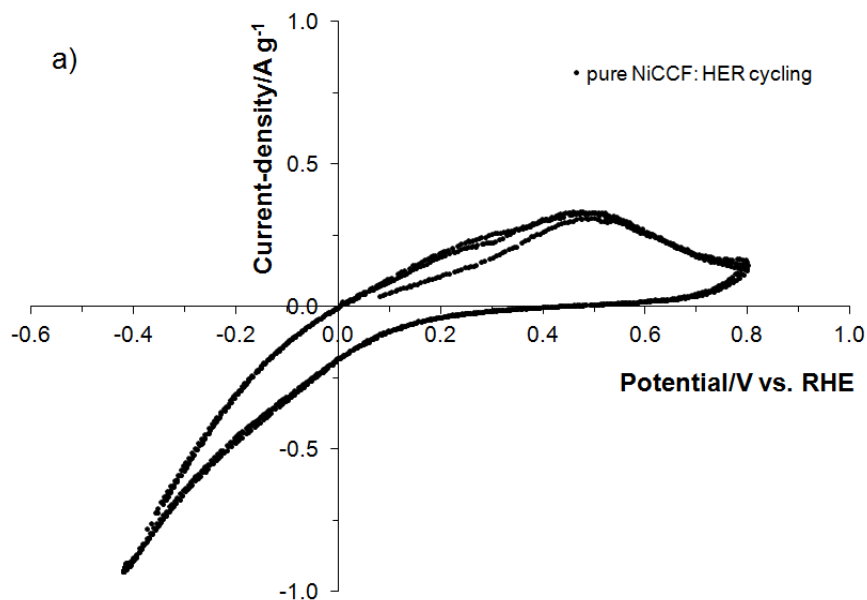

Figure 4. $-\log R_{ct}$ vs. overpotential relationship, obtained for the HER in 0.1 M NaOH solution, for the stated NiCCF-based tow electrodes. Symbols represent experimental results and lines are data fits.

Moreover, the Pd-modified NiCCF catalyst tow is characterized by substantially increased values of double-layer capacitance parameter (*ca.* 4.4 and 6.3 times at -50, and -400 mV, respectively), as compared to those of "as received" Toho-Tenax nickel-coated carbon fibre electrode (Table 1). Thus, electrodeposition of a very small amount of palladium (see Figs. 1a and 1b again) onto the NiCCF tow results in a major modification of the electrochemically active surface area for this fibre material. Also, significant reduction of the C_{dl} parameter from 755,873 μF g^{-1}s$^{\varphi1-1}$ at -50 mV to 509,206 μF g^{-1}s$^{\varphi1-1}$ at -400 mV for the Pd-modified NiCCF material is presumably caused by partial blocking of the electrochemically active electrode surface by *in-situ* formed hydrogen bubbles. Furthermore, the dimensionless φ_1 and φ_2 parameters of the CPE circuit (Table 1 and Fig. 3) varied between 0.61-0.99 and 0.44-0.97, correspondingly.
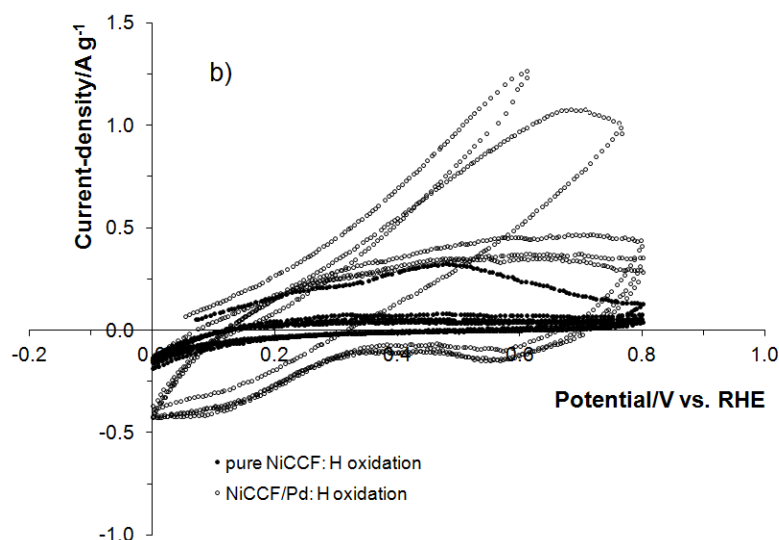
Interestingly, the recorded HER catalytic effect, achieved by Pd modification in alkaline medium, was much less significant than that recently presented for an analogous catalyst system in sulphuric acid solution in Ref. 24. The above could most likely result from small, but inevitable differences in distribution homogeneity and surface deposition level of Pd, achieved on individual NiCCF tow samples.

3.3. Cyclic voltammetry behaviour of pure and Pd-modified NiCCF electrodes in 0.1 M NaOH

An anodic oxidation peak (centred at *ca.* 0.50 V) appears when the voltammetric sweep for an "as received" NiCCF tow electrode is extended over the potential range for the HER (see Fig. 5a).

Figure 5. a) Cyclic voltammogram for "as received" Toho-Tenax 12K50 NiCCF tow electrode in 0.1 M NaOH, recorded at a sweep rate of 50 mV s^{-1} including the potential range, where the HER takes place (*HER cycling*). b) Cyclic voltammograms for "as received" and Pd-modified Toho-Tenax 12K50 NiCCF tow electrodes in 0.1 M NaOH, recorded just after the HER potential cycling, at a sweep rate of 50 mV s^{-1} for potentials positive to the HER range (*H oxidation*).

Then, when the potential range for cycling is limited to potentials positive to the H$_2$ reversible potential, this oxidation peak gradually disappears from the CV profile, which can clearly be seen in Fig. 5b. Similar, although much more pronounced (evidenced through significantly higher current-densities) effect can be observed in Fig. 5b for a palladium-modified NiCCF tow electrode. The above-

recorded anodic oxidation phenomenon corresponds to hydrogen oxidation reaction (HOR), a result of nickel-hydride formation (especially important for Pd) upon cathodic evolution of hydrogen [26-28].

4. CONCLUSIONS

Electrodeposition of palladium at nearly trace amount (*ca.* 1.5 wt.% Pd) on the surface of 12,000-filament nickel-coated carbon fibre tow electrode significantly enhanced catalytic activity of NiCCF baseline material towards cathodic evolution of hydrogen in NaOH solution. The above is primarily related to superior catalytic activity of Pd towards HER, in addition to the resultant, substantial extension of electrochemically active surface area of NiCCF catalyst material. In addition, both NiCCF tow entities exhibited electrochemical impedance behaviour characteristic of a porous electrode structure with two partial semicircles being observed in the Nyquist impedance spectra.

In conclusion, obtained substantial enhancement of catalytic HER behaviour for palladium-modified (at nearly trace amount of Pd), commercially available NiCCF material indicates significant opportunities for this type of cathodes in commercial alkaline water electrolysers.

References

1. B.E. Conway and B.V. Tilak, *Adv. Catalysis*, 38 (1992) 1.
2. J. Barber, S. Morin and B.E. Conway, *J. Electroanal. Chem.*, 446 (1998) 125.
3. J.H. Barber and B.E. Conway, *J. Electroanal. Chem.*, 461 (1999) 80.
4. B.E. Conway and B.V. Tilak, *Electrochim. Acta*, 47 (2002) 3571.
5. A.C.D. Angelo, *Int. J. Hydrogen Energy*, 32 (2007) 542.
6. N.M. Markovic, S.T. Sarraf, H.A. Gasteiger and P.N. Ross, *J. Chem. Soc. Faraday Trans.*, 92 (1996) 3719.
7. J.Y. Huot and L. Brossard, *Int. J. Hydrogen Energy*, 12(12) (1987) 82.
8. H.E.G. Rommal and P.J. Morgan, *J. Electrochem. Soc.*, 135(2) (1988) 343.
9. D.M. Soares, O. Teschke and I. Torriani, *J. Electrochem. Soc.*, 139(1) (1992) 98.
10. C. Hitz and A. Lasia, *J. Electroanal. Chem.*, 500 (2001) 213.
11. J.Y. Huot and L. Brossard, *J. Appl. Electrochem.*, 18 (1988) 815.
12. Y.M. Wu, W.S. Li, X.M. Long, F.H. Wu, H.Y. Chen, J.H. Yan and C.R. Zhang, *J. Power Sources*, 144 (2005) 338.
13. G. Sheela, M. Pushpavanam and S. Pushpavanam, *Int. J. Hydrogen Energy*, 27 (2002) 627.
14. T. Burchardt, *Int. J. Hydrogen Energy*, 25 (2000) 627.
15. A. Królikowski and A.Wiecko, *Electrochim. Acta*, 47 (2002) 2065.
16. K. Hashimoto, T. Sasaki, S. Meguro and K. Asami, *Mater. Sci. Eng. A*, 375-377 (2004) 942.
17. M. Mitov, E. Chorbadzhiyska, R. Rashkov and Y. Hubenova, *Int. J. Hydrogen Energy*, doi:10.1016/j.ijhydene.2012.02.102.
18. M.A. Dominguez-Crespo, A.M. Torres-Huerta, B. Brachetti-Sibaja and A. Flores-Vela, *Int. J. Hydrogen Energy*, 36 (2011) 135.
19. M.A. Dominguez-Crespo, E. Ramirez-Meneses, A.M. Torres-Huerta, V. Garibay-Febles and K. Philippot, *Int. J. Hydrogen Energy*, 37 (2012) 4798.
20. R. Solmaz, A. Gundogdu, A. Doner and G. Kardas, *Int. J. Hydrogen Energy*, 37 (2012) 8917.
21. B. Pierozynski and L. Smoczynski, *J. Electrochem. Soc.*, 156(9) (2009) B1045.

22. B. Pierozynski, *Int. J. Electrochem. Sci.*, 6 (2011) 63.
23. B. Pierozynski and T. Mikolajczyk, *Int. J. Electrochem. Sci.*, 7 (2012) 9697.
24. B. Pierozynski, *Int. J. Hydrogen Energy*, doi: 10.1016/j.ijhydene.2013.04.092.
25. J.R. Macdonald, Impedance spectroscopy, emphasizing solid materials and systems. New York: John Wiley & Sons (1987).
26. B.E. Conway and G. Jerkiewicz, *Electrochim. Acta*, 45 (2000) 4075.
27. T. Imokawa, K.J. Williams and G. Denuault, *Anal. Chem.*, 78 (2006) 265.
28. D.S. Dos Santos and P.E.V. De Miranda, *Int. J. Hydrogen Energy*, 23(11) (1998) 1011.